Published in final edited form as:
Cancer Res. 2020 December 01; 80(23): 5317–5329. doi:10.1158/0008-5472.CAN-20-2116.

Fibroblast-derived IL-33 facilitates breast cancer metastasis by modifying the immune microenvironment and driving type-2 immunity

Ophir Shani[1], **Tatiana Vorobyov**[1], **Lea Monteran**[1], **Dor Lavie**[1], **Noam Cohen**[1], **Yael Raz**[1], **Galia Tsarfaty**[2], **Camila Avivi**[3], **Iris Barshack**[3], **Neta Erez**[1]

[1]Department of Pathology, Sackler Faculty of Medicine, Tel Aviv University, Tel Aviv 69978, Israel

[2]Department of Diagnostic Imaging, Chaim Sheba Medical Center, affiliated with Sackler Faculty of Medicine, Tel Aviv University, Tel Aviv 69978, Israel

[3]Department of Pathology, Sheba Medical Center, Tel Hashomer, affiliated with Sackler Faculty of Medicine, Tel Aviv University, Tel Aviv, Israel

Abstract

Lungs are one of the main sites of breast cancer metastasis. The metastatic microenvironment is essential to facilitate growth of disseminated tumor cells. Cancer-associated fibroblasts (CAF) are prominent players in the microenvironment of breast cancer. However, their role in the formation of a permissive metastatic niche is unresolved. Here we show that IL-33 is upregulated in metastases-associated fibroblasts in mouse models of spontaneous breast cancer metastasis and in breast cancer patients with lung metastasis. Upregulation of IL-33 instigated type-2 inflammation in the metastatic microenvironment, and mediated recruitment of eosinophils, neutrophils and inflammatory monocytes to lung metastases. Importantly, targeting of IL-33 *in vivo* resulted in inhibition of lung metastasis and significant attenuation of immune cell recruitment and type-2 immunity. These findings demonstrate a key function of IL-33 in facilitating lung metastatic relapse by modulating the immune microenvironment. Our study shows a novel interaction axis between CAF and immune cells and reveals the central role of CAF in establishing a hospitable inflammatory niche in lung metastasis.

Keywords

Cancer-associated fibroblasts; Breast cancer; Lung metastasis; IL-33; Inflammation

Correspondence to: Neta Erez.

*Corresponding Author: Neta Erez, netaerez@tauex.tau.ac.il, Telephone: +972-3-6408689.

Conflict of interests
The authors declare no competing financial interests.

Author contribution
OS conceived and carried out experiments, analyzed data and generated figures; OS, TV, LM, CA and DH carried out experiments; GT performed CT imaging analysis, NC was involved in data analysis and discussions; IB contributed essential resources; NE designed and supervised the study; NE and OS wrote the manuscript.

Europe PMC Funders Author Manuscripts

Europe PMC Funders Author Manuscripts

Introduction

Mortality from breast cancer is almost exclusively a result of tumor metastasis to distant organs. Advanced metastatic cancers are mostly incurable and available therapies only prolong life to a limited extent. It has become clear in recent years that the metastatic microenvironment plays a crucial role in enabling the growth of disseminated tumor cells (1). Changes in the metastatic niche precede metastases formation, and drive the formation of a hospitable microenvironment in multiple organs, mediated by modifications of the immune milieu and of the extracellular matrix (2). Lungs are one of the most common sites of breast cancer metastasis. Various immune cell populations were shown to be functionally important in facilitating breast cancer pulmonary metastasis (3–6). Specifically, instigation of type-2 immunity was shown to be associated with pulmonary metastasis in multiple cancer types (7,8). However, the mechanisms underlying these changes in the lung metastatic niche are largely unresolved.

IL-33 is a member of the IL-1 family of cytokines (9). It belongs to a group of alarmin molecules and its release from cells during cell injury instigates an inflammatory tissue damage response (10,11). Under physiological conditions, IL-33 is constitutively expressed in epithelial, endothelial and fibroblastic cells, and is found in the nucleus (12,13). During inflammation or other types of stress, IL-33 is upregulated and released from necrotic or damaged cells (11). IL-33 is an inducer of type-2 immune responses, implicated in multiple pathologies including allergic, fibrotic, infectious, and chronic inflammatory diseases (14). In lungs, IL-33 was shown to be involved in mediating Th2 immune responses in models of allergic asthma (15,16). In cancer, IL-33 was demonstrated to have tumor-promoting as well as tumor-inhibiting functions in several tumor types (17). However, the role of IL-33 in the context of the metastatic niche is largely unknown.

Cancer-associated fibroblasts (CAFs) are a heterogeneous population of stromal cells in the microenvironment of solid tumors. In some cancer types, including breast carcinomas, CAFs are the most prominent stromal cell type, and their abundance correlates with worse prognosis (18). We previously demonstrated a novel role for CAFs in mediating tumor-promoting inflammation in mouse and human carcinomas (19–21). Importantly, there were profound changes in the expression of pro-inflammatory genes in fibroblasts isolated from metastases-bearing lungs (22,23). However, very little is known about the role of fibroblasts during the complex process of metastases formation, and their interactions with immune cells in the metastatic microenvironment.

Here we show that IL-33 is upregulated in the lung metastatic microenvironment, and that CAFs are the main cellular source of IL-33 during breast cancer metastasis. Functionally, we found that stromal-derived IL-33 drives type-2 inflammation and recruitment of multiple immune cell types to the lung microenvironment, which facilitated lung metastasis.

Materials and Methods

Mice

All experiments involving animals were approved by the Tel Aviv University Institutional Animal Care and Use Committee. MMTV-PyMT 634Mul/J transgenic mice were from Dr. Lisa Coussens. FVB/n;*Col1a1*-YFP mice were a gift from Dr. Gustavo Leone. MMTV-PyMT were crossed with FVB/n;*Col1a1*-YFP mice to create MMTV-PyMT;*Col1a1*-YFP double-transgenic mice as we previously described (22). BALB/c;*Col1a1*-YFP were generated in our lab. Non-transgenic BALB/c mice were purchased from Harlan, Israel. All animals were maintained at the Tel Aviv University Specific Pathogen Free facility.

Cancer cell lines and primary lung fibroblasts

Met-1 cells were received from Dr. Jeffrey Pollard. 4T1 cells were received from Dr. Zvi Granot. Tumor cell culture and CM preparation were performed as previously described (21). Cell lines were not authenticated in our laboratory. All cell lines were routinely tested for mycoplasma using the EZ-PCR-Mycoplasma test kit (Biological Industries; 20-700-20). Primary lung fibroblasts were isolated from lungs of FVB/n or BALB/c mice following dissociation of lung tissue as previously described (21). All experiments were performed with low passage (p2-4) fibroblasts.

Lung homogenate supernatant

Lungs were perfused with 10ml PBS, harvested, and placed in 70μm cell strainers in 50ml tube containing RPMI1640 media. Lungs were homogenized using a syringe plunger, and centrifuged 5min at 500g. Supernatants were collected and filtered through 0.45μm filters.

Broncho-alveolar lavage fluid (BALF)

Mice bearing lung metastases or normal controls were euthanized, and 3X500μl of PBS was injected intra-trachea and recollected into the syringe. BALF was concentrated using Amicon Ultra-0.5 Centrifugal Filter Units with Ultracel-10 membrane (Merck Millipore, UFC501024).

Enzyme-linked immunosorbent assay (ELISA)

ELISA for IL-33 in lung homogenate supernatant or in BALF was performed using Mouse IL-33 Quantikine ELISA Kit (R&D Systems, M3300).

BM-derived neutrophils and monocyte isolation

Bone marrow cells were isolated from the femur and tibia of 10-weeks old mice. Neutrophils and monocytes were separated by density gradient centrifugation, using Histopaque 1119 or 1077 (11191 and 10771, Sigma-Aldrich).

T cells isolation

Spleens were harvested from 10-12 weeks old mice, minced and dissociated. T cells were isolated using Pan T-Cell isolation kitII (130-095-130).

BM-derived eosinophil isolation

Bone marrow from 6wks old mice was loaded using histopaque gradient (10831, Sigma Aldrich) and low-density cells were collected for culture. Cells were cultured in IMDM medium (12440053, Gibco) supplemented with 10% FCS, 100ng/ml recombinant SCF (250-03-50, Peprotech) and 100ng/ml recombinant Flt3 (250-31L, PeproTech) for 4 days. Media was supplemented with 10ng/ml recombinant IL-5 (215-15, PeproTech) for 11 days, changing medium every other day. On day 14, eosinophil purity was analyzed by flow cytometry and cytostaining. >85% was defined as acceptable purity. Differential Quick Staining was performed using KIT DIF STAIN (KALTEK SRL, 1526).

Migration assays

Bone marrow-derived neutrophils (5×10^5), monocytes (5×10^5), T cells (1×10^6), and eosinophils (5×10^5 cells) were placed at the upper chamber of 24-transwell membrane plates (Corning; CA-3415, CLS3421 or CA-3422). Migration assays were performed with 5μm pore (neutrophils), 8μm pore (monocytes) or 3μm pore transwell inserts (T cells and eosinophils). Lung homogenate supernatant from normal or metastases-bearing lungs was placed at the bottom chamber. Neutralizing anti-IL-33 antibody (0.2μg/ml AF3626, R&D systems) was added and migrated cells were counted by cell counter.

Immunostaining

Tissue sections—Lungs were injected intratracheally with 600μL O.C.T (BN62550, Tissue-Tek), harvested, washed in PBS and embedded in O.C.T on dry ice. Serial sections were obtained to ensure equal sampling of the examined specimens (8μm trimming).

Immunofluorescence—Staining was performed as previously described (21). Anti-mouse IL-33 antibody (2μg/ml), anti-YFP antibody (0.5μg/ml, ab6556 abcam), RedX–conjugated secondary antibody (705-295-147, Jackson ImmunoResearch Laboratories) and 488–conjugated secondary antibody (A21206, Invitrogen) were used. Slides were visualized using Leica SP5 microscope. Brightness and contrast were adjusted equally in all images. Quantitative analyses were performed using ImageJ Software. Metastases-bearing lung quantification was divided to fields of view (FOV) without metastases (Mets adj.) and FOV with Metastases (Mets).

H&E staining—H&E staining was performed as previously described (21). Images were obtained using the Leica Aperio VERSA slide scanner.

Orthotopic tumor transplantations

Tumor cells (2×10^5 4T1 cells) were suspended in PBS and mixed 1:1 with Matrigel (BD Biosciences, 354230). 100ul of cell mixture was injected into the right inguinal mammary glands of 8-weeks-old female BALB/c mice. Tumors were resected 3 weeks following the injection.

In vivo experiments

IL-33 inhibition in vivo—One day following tumor resection mice were injected intraperitoneally with 5μg/mouse of anti-IL-33 antibody, or with 5μg isotype control antibody (AB-108-C R&D systems). For eosinophil ablation, mice were injected with 15μg/mouse anti-SiglecF antibody (MAB17061, R&D systems), or with 15μg/mouse isotype control (MAB006R, R&D systems), alone or in combination with anti-IL-33 as indicated in Figure S4. Injections were performed twice weekly to a total of 5 injections. Mice were euthanized one day after the last injection.

Quantification of lung metastatic load

CT imaging and quantification—CT imaging of lungs was performed one day after the last injection, prior to euthanizing the mice. Images were analyzed by a specialist radiologist. Metastasis quantification included counting the total number of metastases, and measurement of metastatic area and volume.

H&E quantification—Quantification of lung metastatic load was performed by analyzing the number of metastatic nodules per section or by evaluating the metastatic area per section normalized to lung area per section using ImageScope.

Human IL-33 staining

Human patient samples were collected with written informed consent and processed at the Sheba Medical Center, Israel, in accordance with recognized ethical guidelines, under an approved Institutional Review Board (IRB) (3112-16). Tissue sections stained for IL-33 (AF3625, R&D systems) were analyzed by an expert pathologist. Images were scanned at X20 magnification using the Leica Aperio VERSA slide scanner. Analysis was performed using ImageScope software. In each slide, 5-10 areas of metastases and 5-10 normal areas were arbitrarily selected, and quantified for IL-33+ cells.

FACS sorting

Single cell suspensions of normal lungs and metastases-bearing lungs isolated from FVB/n;*Col1a1*-YFP, MMTV-PyMT;Col1a1-YFP or BALB/c;Col1a1-YFP mice were stained and isolated as previously described (22).

Flow cytometry analysis

Immune cell infiltration to lungs and ST2 analysis—Single cell suspensions of normal lungs and metastases-bearing lungs were were incubated with anti-mouse CD16/CD32 (eBioscience, 16-0161-82) for 15 min, followed by staining with the following anti-mouse antibodies: anti-CD45-BV650 (Biolege419nd, BLG-103151), anti-CD11b-PeCy7 (Biolegend, BLG-101216), anti-CD11c-PerCP-Cy5.5 (eBioscience, 45-0114), anti-SiglecF-APC-R700 (BD bioscience, BD565183), anti-Ly6G-APC (Biolegend, 127614), anti-Ly6C-FITC (Biolegend, 128006), anti-NKp46-PeCy7 (Biolegend, BLG-137618), anti-B220-PerCP-Cy5.5 (Biolegend, BLG-103236), anti-CD4-APC-Cy7 (Biolegend, BLG-100413), anti-CD8a-APC (Biolegend, BLG-100712), anti-CD3-FITC (eBioscience, 11-0031), anti-ST2-PE (Biolegend, 145303) and DAPI (Molecular Probes; D3571). Specificity of staining

was validated by appropriate isotype control per each antibody and by fluorescence-minus-one (FMO) method. Immune populations were defined based on previous studies of lung immune populations (24,25).

Eosinophil purity in vitro—Cultured bone marrow cells were stained with anti-SiglecF-APC-R700 and anti-CCR3-FITC (eBioscience, FAB729F) and analyzed for eosinophil purity. Flow cytometric analyses were performed using CytoFLEX Flow Cytometer (Beckman Coulter). Data analysis was performed with the Kaluza Flow Analysis software (Beckman Coulter).

RNA isolation and qRT-PCR

RNA from sorted cells was isolated using the EZ-RNAII kit (20-410-100, biological industries). RNA from *in vitro* experiments and from total lungs was isolated using the PureLink™ RNA Mini Kit (Invitrogen; 12183018A). cDNA synthesis was conducted using qScript cDNA Syntesis kit (Quanta; 95047-100). qRT-PCR were conducted using PerfeCTa SYBR Green Fastmix ROX (Quanta; 95073-012). Expression results were normalized to *Gusb, Gapdh* or *Ubc* and to controls. RQ ($2^{-\Delta\Delta Ct}$) was calculated.

RNAseq analysis

Expression analysis of inflammatory genes was based on a dataset we previously described (GSE128999 (23)). Go-term enrichment analysis was performed on genes overexpressed in metastases-associated fibroblasts as compared with normal lung fibroblasts (Fold change>1.5, adjusted p-value<0.05) using the STRING platform. Heatmap was generated based on gene expression Z-scored per gene derived from RNAseq data.

Human data

Stromal and epithelial expression of *IL33* were analyzed in human breast cancer based on a publicly available datasets GSE14548 (26), GSE9014, GSE12622 (27) and GSE88715 (28). Metastatic site expression of IL-33 were analyzed in human breast cancer based on a publicly available dataset GSE14020 (29,30).

Statistical analysis

Statistical analyses were performed using GraphPad Prism software. All tests were two-tailed unless otherwise stated. Bar graphs represent mean and SD of at least 3 separate biological repeats. P-value of ≤0.05 was considered statistically significant.

Results

IL-33 is upregulated in metastases-associated fibroblasts at the lung metastatic microenvironment

We previously characterized the co-evolution of metastases-associated fibroblasts in breast cancer lung metastases by profiling their transcriptome at distinct metastatic stages, using fibroblasts that were isolated from MMTV-PyMT;*Col1a*-YFP transgenic mice, in which all fibroblasts are fluorescently labeled (23). Utilizing GO analysis, we found that an inflammatory gene signature was highly enriched in fibroblasts isolated from metastases-

associated fibroblasts (MAF) in lung macrometastases as compared with normal lung fibroblasts (NLF) (Fig. 1A). Specifically, analysis of the data revealed that one of the genes that were highly upregulated in MAF is *Il33.*

IL-33 is a stromal cytokine with multiple known functions in both physiological and pathophysiological settings. While IL-33 was implicated in breast cancer (31,32), very little is known regarding its role in the metastatic niche, and even less is known about its role in fibroblasts. Intrigued by this finding, we set out to validate the expression of IL-33 in fibroblasts isolated by FACS from spontaneous lung metastases in MMTV-PyMT mice, as well as in an additional mouse model of breast cancer metastasis to lungs, the transplantable 4T1 triplenegative tumor cells, orthotopically injected to BALB/c;Col1a1-YFP mice. The results confirmed that IL-33 is significantly upregulated in MAF (Fig. 1B). Since IL-33 is expressed by various cell types, we next assessed the cellular origin of IL-33 in the lung metastatic niche. To that end, we isolated by FACS immune cells ($CD45^+CD31^-$), endothelial cells ($CD31^+CD45^-$), epithelial/tumor cells ($EpCAM^+CD45^-CD31^-$) or fibroblasts ($YFP^+CD45^-CD31^-EpCAM^-$) from metastases-bearing lungs (Supplementary Fig. S1A). Analysis of *Il33* expression indicated that fibroblasts exhibited the highest expression of *Il33* in both the autochthonous and the transplantable models, suggesting that fibroblasts are the main source of *Il33* in lung metastases (Fig. 1C). Of note, the basal expression of *Il33* was not altered in epithelial cells at the metastatic lung as compared with normal lung (Supplementary Fig. S1B). Interestingly, *in vitro* expression of *Il33* in normal lung fibroblasts was elevated in response to activation with the tumor cell-conditioned medium, suggesting that reprogramming by tumor cell-secreted factors may drive the upregulation of IL-33 in MAF (Fig. 1D). In addition to its intracellular roles, IL-33 functions as a pro-inflammatory/alarmin cytokine (33). To investigate whether secreted/extracellular IL-33 is operative in the lung microenvironment we analyzed IL-33 in lung tissue supernatants of metastases-bearing lungs compared with normal lungs, and in the content of broncho-alveolar lavage fluids (BALF) from normal or metastases-bearing lungs. We found that protein levels of IL-33 were significantly higher in BALF and lung supernatants isolated from metastases-bearing lungs compared with normal controls (Fig. 1E-H). To further assess the expression of IL-33 in the lung metastatic microenvironment, we performed immunofluorescent staining of IL-33 in metastases-bearing lungs and in normal controls. While in normal lungs there was sparse IL-33 expression in lung parenchymal cells, IL-33 was elevated in lungs of mice with metastases, particularly around metastatic lesions. Furthermore, the levels of expression per cell were the highest in stromal cells located within metastatic lesions, compared with cells in lung areas adjacent to metastases or in normal lungs (Fig. 1I,J, Supplementary Fig. S1C). Moreover, co-staining of YFP+ fibroblasts and IL-33 confirmed that IL-33 is almost exclusively expressed by fibroblasts (Figure 1K).

To test the functional importance of these findings, we next asked whether *Il33* expression is correlated with lung metastasis. Quantification of lung metastatic volume by CT imaging in 4T1 injected mice (Fig. 1L) and analysis of *Il33* expression in total lungs, revealed that *Il33* expression significantly correlated with metastatic load (Fig. 1M), implying that fibroblast-derived IL-33 may be functionally important in metastatic progression. Taken together, these results indicate that the expression of IL-33 is specifically upregulated in lung metastases-associated fibroblasts and suggest a role for stromal IL-33 in the lung metastatic niche.

Lung metastases formation is characterized by extensive modifications in the immune milieu

Since tumor metastasis is accompanied by significant changes in the immune microenvironment and IL-33 is a known immune modulator and a driver of type-2 immunity (10), we hypothesized that stromal upregulation of IL-33 mediates changes in the metastatic immune microenvironment. To test this hypothesis, we initially analyzed the expression of multiple cytokines and chemokines that were implicated as *Il33* downstream genes (34), in metastases-bearing lungs or in normal lungs. Analysis of the results confirmed a significant upregulation in the expression of multiple immune related genes (Fig. 2A, Supplementary Fig. S2A). In addition, since IL-33 is known to mediate type-2 inflammation, we analyzed the expression of transcription factors (TF) associated with type-1 (Tbet) and type-2 immunity (Gata3, Foxp3). We found in the 4T1 model, that while the expression of Gata3 and Foxp3 was unchanged, there was a significant downregulation in the expression of Tbet, a TF associated with type-1 immunity and with tumor rejection (Fig. 2B). Interestingly, in the transgenic PyMT model Gata3 was significantly elevated while Tbet was unchanged (Supplementary Fig. S2B), suggesting that different modulations of gene expression are operative to drive transcriptional regulation towards type-2 immunity, in a context-dependent manner. Furthermore, there was a significant positive correlation between the expression of IL-33 and the expression levels of many of the immune-related factors that we analyzed, and a negative correlation with the expression of Tbet (Fig 2C), further implicating IL-33 in modifying the immune microenvironment in lung metastasis.

To assess whether these changes in gene expression are reflected in modifications in the lung immune milieu, we characterized immune cell populations in the microenvironment of metastatic lungs compared with normal lungs. Analysis revealed that the number of immune cells was significantly increased in metastases-bearing lungs, pointing at the massive immune infiltration that accompanies metastases formation (Fig. 2D). To further characterize the immune milieu, we performed a comprehensive flow cytometry analysis in the lung metastatic microenvironment compared with normal controls. Analysis of the results showed significant changes in the composition of immune cell populations in metastases-bearing lungs, in both the transgenic and transplantable models (Fig. 2E, Supplementary Fig. S2C,D). Interestingly, some of the changes in immune cell populations were different between the mouse models: while in the 4T1 model the most striking change was a massive increase in eosinophils, the most prominent change in the PYMT model was in the neutrophil population, suggesting that the specific composition of the immune cell milieu is dependent on the pathological context (Fig. 2E,I). A detailed analysis of immune cell infiltration in the lung metastatic microenvironment revealed that while recruitment of eosinophils, B cells, $CD8^+$ T cells and dendritic cells was model-specific, significant increases in the numbers of neutrophils, inflammatory monocytes and CD4+ T cells were common to both models (Fig. 2F-J). These results reveal the substantial changes in immune cell infiltration and milieu at the metastatic lung, with a great increase in both number and fraction of eosinophils, neutrophils and inflammatory monocytes, suggesting that these cells have a functional role in lung metastasis.

ST2, the IL-33 receptor is highly upregulated in immune cells at the metastatic microenvironment

To test whether stromal IL-33 may affect these changes in the metastatic immune microenvironment, we next analyzed the expression and distribution of ST2, the receptor of IL-33, on various cell populations in lungs. ST2 is known to be expressed by immune cells, but it was also shown to be expressed by stromal cells and tumor cells (35). We analyzed the expression of ST2 on various cell populations isolated by FACS from normal lungs, compared with cells isolated from metastases-bearing lungs of both the MMTV-PyMT transgenic model and the 4T1 transplantable model. We found that ST2 is expressed almost exclusively on CD45+ immune cells (Fig. 3A). Furthermore, the expression of ST2 was upregulated in immune cells isolated from metastases-bearing lungs as compared with normal lungs (Fig 3A-D). To examine which immune cells express ST2, we assessed its expression on different immune sub-populations by flow cytometry analysis. Interestingly, upregulation of ST2 expression was highest on metastases-associated eosinophils, neutrophils, and inflammatory monocytes, which were the cell types most highly recruited into metastatic lungs (Fig. 3E-H). These results further supported our hypothesis that stromal-derived IL-33 may affect the recruitment and/or function of immune cells in the lung metastatic microenvironment.

IL-33 is functionally important for direct recruitment of T cells and eosinophils

To test whether IL-33 is functional in recruitment of eosinophils, neutrophils, monocytes and T cells we analyzed *in vitro* the migration of these cells towards lung supernatants prepared from normal lungs, metastases-bearing lungs or metastases-bearing lungs supplemented with anti-IL-33 (Fig. 4A). Notably, the migration of all the tested immune cell types was significantly enhanced in response to factors in metastases-bearing lungs compared with normal lungs (Fig. 4B-D,F). Interestingly, inhibiting the function of IL-33 in supernatant from metastatic lungs, by adding anti-IL-33 antibodies significantly inhibited the migration of T cells (Fig. 4D) and of eosinophils (Fig. 4E,F, Supplementary Fig. S3A,B), suggesting a direct role for IL-33 in the recruitment of these cell populations to lungs. However, while there was a trend towards attenuation of migration, inhibition of IL-33 did not significantly inhibit the migration of monocytes and neutrophils (Fig. 4B,C). This discrepancy may be explained by the fact that some of the IL-33 downstream genes that were upregulagted in metastatic lungs such as *Ccl2* and *Cxcl1* (Fig. 2A,C) are known chemoattractants for monocytes and neutrophils, and inhibition of IL-33 *in vitro* did not abrogate their function in the lung supernatant. Taken together, these results suggest that MAF-derived IL-33 mediates the recruitment of immune cells to the lung metastatic microenvironment.

Inhibition of IL-33 attenuates lung metastases, and tempers type-2 immunity in the metastatic lung

To elucidate the functional role of IL-33 in lung metastasis *in vivo,* we performed experiments to inhibit IL-33 in an adjuvant setting. The autochthonous growth of mammary tumors in the transgenic MMTV-PyMT mouse model is characterized by formation of multiple primary tumors that are non-resectable, and therefore do not mimic the clinical settings of breast cancer metastatic relapse. To recapitulate the clinical setting, we utilized

for these experiments the 4T1 model of spontaneous lung metastasis following resection of a transplanted mammary tumor. Tumor cells were injected orthotopically to the mammary gland, and surgically resected after 3 weeks, when they reached a size of ~0.3cm^3. Following tumor resection, we treated mice with anti-IL-33 antibody or isotype control (Fig. 5A). Lung metastatic load was assessed intra-vitally by CT imaging (Fig. 5B-D), followed by H&E staining of lung tissue sections (Fig. 5E-G). Analysis of the results revealed a striking decrease in the number of metastatic foci as well as in the size of metastatic lesions in mice treated with anti-IL-33 antibody, implying that IL-33 is functionally important in the formation of breast cancer lung metastasis.

Seeking to get mechanistic insight on the metastases-promoting function of IL-33, and based on our findings that lung metastases are characterized by significant recruitment of immune cells and upregulation of ST2 expression and type-2 immunity, we next analyzed the immune cell composition in lungs of mice treated with anti-IL-33 as compared with controls. We found that targeting IL-33 *in vivo* resulted in a strong inhibition of immune cell recruitment to metastatic lungs (Fig. 5H).

Since eosinophils were the most strikingly recruited population to lung metastases of 4T1 injected mice (Figure 2E,I), and inhibition of IL-33 attenuated their recruitment, we hypothesized that eosinophils may be functionally important downstream of IL-33 in metastasis promotion. To test whether eosinophil ablation would mimic IL-33 inhibition, 4T1-injected mice were treated following resection of the primary tumor with with anti-SiglecF, to eliminate eosinophils, or with anti-IL-33, or both (Supplementary Fig. S4A). Analysis of eosinophil presence in lungs revealed that inhibition of IL-33 was comparable to anti-SiglecF treatment in reducing eosinophil infiltration to lungs, further confirming the essential role of IL-33 in eosinophil recruitment *in vivo* (Supplementary Fig. S4B,C). However, analysis of metastatic burden revealed that inhibition of IL-33 was more efficient in attenuating metastasis than eosinophil elimination (Supplementary Fig. S4D-F). Moreover, the combined treatment of anti-IL-33 and anti-SiglecF had no additive effect on metastatic incidence or burden compared with the single treatment. These results suggest that the role of IL-33 in promoting metastasis is pleotropic, and is not eosinophil-dependent.

To further assess the immune-modulating effect of IL-33, we analyzed the expression of multiple IL-33 downstream chemokines and cytokines, in lungs of mice treated with anti-IL-33, and found that inhibition of IL-33 resulted in a significant decrease in the expression of type-2 immunity related genes. We also analyzed the expression of IFNγ and TNFα, known to be related to type-1 immunity, and found that targeting IL-33 did not affect their expression (Fig. 5I). Notably, *Cxcl1,* a known neutrophil chemoattractant, was unchanged by IL-33 inhibition, in agreement with our finding that neutrophil infiltration to lungs was not affected by IL-33 inhibition (Fig. 5H). Moreover, analysis of the expression of the TFs *Gata3, Foxp3 and Tbet* in response to IL-33 inhibition revealed a significant attenuation of the expression of Gata3, known to regulate type-2 immune response, with no change in the expression of *Foxp3* or *Tbet* (Fig. 5J). Taken together, these findings functionally implicate IL-33 in facilitating lung metastatic relapse and in mediating metastases-promoting type-2 immunity in lungs.

IL-33 is upregulated in the stroma of breast cancer primary tumors and lung metastases in human patients

Finally, we asked whether upregulation of stromal IL-33 is also operative in human primary breast cancer and lung metastasis. To address this question, we analyzed IL-33 expression in human breast tumors from several datasets (26–28). Initially, we analyzed the expression of *IL33* in normal stroma compared with tumor-associated stroma and found that *IL33* is significantly upregulated in the stromal compartment (Fig. 6A). Moreover, analysis of IL33 expression in paired tumor and stromal samples from the same patient confirmed higher expression of *IL33* in the stroma (Fig. 6B). To test whether the expression of *IL33* changes with tumor progression, we compared its expression in epithelial and stromal cells derived from different tumor grades. Interestingly, *IL33* expression was significantly upregulated in the stroma of higher-grade tumors (Fig. 6C), suggesting that stromal upregulation of IL-33 may be associated with tumor progression.

We further asked whether upregulation of IL-33 is characteristic of human breast cancer lung metastasis. To that end, we analyzed the expression of IL-33 in a publicly available dataset of gene expression in the most common anatomical sites of breast cancer metastases: bone, brain, liver and lungs (29,30). Strikingly, the expression of IL-33 was significantly higher in lung metastasis compared with other metastatic sites (Fig. 6D), suggesting a specific role for IL-33 at the lung metastatic niche.

To further validate our findings, we performed histopathological analysis in a cohort of breast cancer patients with lung metastasis. Immunohistochemistry for IL-33 in lung tissue sections revealed that IL-33 expressing cells were highly increased in lung metastases, compared with normal lung tissue (Fig. 6E-G). Notably, the expression of IL-33 in human lung metastases was limited to the stromal compartment, similarly to our observation in murine lung metastases. Thus, stromal IL-33 is upregulated in both human breast cancer primary tumors and lung metastases.

Discussion

In this study we showed that IL-33 is upregulated in metastases-associated fibroblasts in two different mouse models of spontaneous breast cancer metastasis to lungs- a transgenic model (MMTV-PyMT), and a transplantable model (4T1), following resection of the primary tumor. Moreover, analysis of lung metastases from breast cancer patients revealed that stromal upregulation of IL-33 is also operative in human disease. We further demonstrated that IL-33 upregulation in the lung metastatic niche was associated with recruitment of immune cells and with modulating the cytokine and chemokine milieu in lungs towards type-2 inflammation. These changes were abrogated following inhibition of IL-33. Importantly, targeting of IL-33 *in vivo* by treating mice with neutralizing antibodies resulted in striking inhibition of lung metastasis, indicating a central role for fibroblast-derived IL-33 in facilitating lung metastatic relapse, via modulating the metastatic immune microenvironment.

Our findings indicate that fibroblasts are the main source of IL-33 in lung metastasis. Stromal cells were shown to modulate immunity and inflammation via IL-33 in

physiological conditions (36,37). In primary tumors, stromal-derived IL-33 was implicated in tumor promotion by enhancing tumor cell growth and invasion (38,39), and by affecting the recruitment and function of macrophages (40,41). Our findings demonstrate that stromal-derived IL-33 at the metastatic site facilitates metastasis by recruitment of multiple immune cells and by modulating the lung immune microenvironment. Interestingly, we previously showed that CAFs can function as sensors of damage-associated molecular patterns (DAMPs) in breast tumors (21). Our current findings add another layer to this novel role of fibroblasts and show that tissue damage responses mediated by CAF secretion of the alarmin IL-33 play an important role in facilitating metastasis.

By quantifying the alterations in cytokines and chemokines in lung metastasis, we found striking upregulation in the expression of multiple type-2 immunity mediators in lung metastasis, which was abolished when we inhibited IL-33. Notably, IL-33-associated changes in some TFs (Gata3, but not Tbet) suggested that IL-33 may directly affect the expression of type-2 immunity related factors. Moreover, we analyzed the immune cell milieu in lung metastasis and found a prominent increase in multiple immune cell populations including eosinophils, T cells and inflammatory monocytes. Indeed, we found that immune cell infiltration was abolished when IL-33 was inhibited *in vivo,* suggesting a central role for stromal-derived IL-33 in recruitment of these cell types. IL-33 was previously implicated in affecting eosinophil recruitment and maturation (42), as well as recruitment and reprogramming of macrophages and dendritic cells towards an immunosuppressive function in primary tumors (43). We showed that this is also operative in metastasis. Interestingly, while eosinophil recruitment was IL-33 dependent, their ablation was not sufficient to inhibit lung metastasis, suggesting that the role of IL-33 in promoting metastasis is not restricted to a single downstream cell type. Thus, by performing a comprehensive analysis of the immune milieu at the metastatic microenvironment, followed by functional *in vivo* experiments, our findings add a new dimension to the formation of a hospitable metastatic niche by revealing a central role for CAF-derived IL-33 in mediating the recruitment of multiple immune cell types to lung metastasis, and by driving type-2 inflammation.

IL-33 has a controversial role in cancer, with studies showing tumor-promoting or tumor-inhibitory functions in various cancer types (44,45). Notably, a protective role for IL-33 was mostly demonstrated in studies in which IL-33 was exogenously administered or overexpressed in tumor cells (46–48), indicating that the source of IL-33 and the physiological context are of critical importance to its function. Moreover, studies showing tumor-promoting roles for IL-33 mostly focused on primary tumor growth. Our study demonstrates for the first time in a clinically relevant model of spontaneous lung metastasis, following surgical resection of the primary tumor, that fibroblast-derived IL-33 plays a functional role in the lung metastatic niche.

Notably, our analysis of IL-33 expression in human breast cancer metastasis indicated that upregulation of IL-33 is specific for lung metastases. Taken together with our results in mouse models, these findings suggest that targeting IL-33 may be beneficial for inhibiting lung metastatic relapse of breast cancer. Targeting of IL-33 was tested for the treatment of asthma, chronic obstructive pulmonary disease (COPD) and peanut allergy (49).

Interestingly, allergen-induced pulmonary inflammation was shown to enhance lung colonization by circulating tumor cells in a mouse model of experimental metastasis. Moreover, analysis of a clinical breast cancer database revealed higher incidence of lung metastasis in asthmatic patients as compared with non-asthmatic patients (50). Thus, adjuvant targeting of IL-33, limiting pulmonary inflammation, may be beneficial for breast cancer patients with pre-existing pulmonary disease.

In summary, our study reveals a novel interaction axis between fibroblasts and immune cells in the lung metastatic microenvironment, mediated via CAF-derived IL-33 that establishes a hospitable inflammatory niche, by driving type-2 inflammation. Our findings suggest that targeting the IL-33 pathway may offer therapeutic benefit to prevent or treat lung metastasis.

Supplementary Material

Refer to Web version on PubMed Central for supplementary material.

Acknowledgements

This research was supported by grants to NE from the European Research Council (ERC) under the European Union's Horizon 2020 research and innovation programme (grant agreement No. 637069 MetCAF), from the Israel Science Foundation (#1060/18), the Emerson Collective, and the Israel Cancer Research Fund (ICRF Project Grant). The authors would like to thank Sharon Grisaru for her assistance with staining of eosinophils and Prof. Ariel Munitz for critical reading and useful discussion of the manuscript.

References

1. Quail DF, Joyce JA. Microenvironmental regulation of tumor progression and metastasis. Nature medicine. 2013; 19(11):1423–37.
2. Peinado H, Zhang H, Matei IR, Costa-Silva B, Hoshino A, Rodrigues G, et al. Premetastatic niches: organ-specific homes for metastases. Nature reviews Cancer. 2017; 17(5):302–17. [PubMed: 28303905]
3. Albrengues J, Shields MA, Ng D, Park CG, Ambrico A, Poindexter ME, et al. Neutrophil extracellular traps produced during inflammation awaken dormant cancer cells in mice. Science. 2018; 361(6409)
4. Coffelt SB, Kersten K, Doornebal CW, Weiden J, Vrijland K, Hau CS, et al. IL-17-producing gammadelta T cells and neutrophils conspire to promote breast cancer metastasis. Nature. 2015; 522(7556):345–8. [PubMed: 25822788]
5. DeNardo DG, Barreto JB, Andreu P, Vasquez L, Tawfik D, Kolhatkar N, et al. CD4(+) T cells regulate pulmonary metastasis of mammary carcinomas by enhancing protumor properties of macrophages. Cancer cell. 2009; 16(2):91–102. [PubMed: 19647220]
6. Fridlender ZG, Albelda SM, Granot Z. Promoting metastasis: neutrophils and T cells join forces. Cell Res. 2015; 25(7):765–6. [PubMed: 26138787]
7. Kobayashi M, Kobayashi H, Pollard RB, Suzuki F. A pathogenic role of Th2 cells and their cytokine products on the pulmonary metastasis of murine B16 melanoma. J Immunol. 1998; 160(12):5869–73. [PubMed: 9637498]
8. Zhang Q, Qin J, Zhong L, Gong L, Zhang B, Zhang Y, et al. CCL5-Mediated Th2 Immune Polarization Promotes Metastasis in Luminal Breast Cancer. Cancer research. 2015; 75(20):4312–21. [PubMed: 26249173]
9. Schmitz J, Owyang A, Oldham E, Song Y, Murphy E, McClanahan TK, et al. IL-33, an interleukin-1-like cytokine that signals via the IL-1 receptor-related protein ST2 and induces T helper type 2-associated cytokines. Immunity. 2005; 23(5):479–90. [PubMed: 16286016]

10. Mantovani A, Dinarello CA, Molgora M, Garlanda C. Interleukin-1 and Related Cytokines in the Regulation of Inflammation and Immunity. Immunity. 2019; 50(4):778–95. [PubMed: 30995499]
11. Rider P, Voronov E, Dinarello CA, Apte RN, Cohen I. Alarmins: Feel the Stress. J Immunol. 2017; 198(4):1395–402. [PubMed: 28167650]
12. Moussion C, Ortega N, Girard JP. The IL-1-like cytokine IL-33 is constitutively expressed in the nucleus of endothelial cells and epithelial cells in vivo: a novel 'alarmin'? PloS one. 2008; 3(10) e3331 [PubMed: 18836528]
13. Pichery M, Mirey E, Mercier P, Lefrancais E, Dujardin A, Ortega N, et al. Endogenous IL-33 is highly expressed in mouse epithelial barrier tissues, lymphoid organs, brain, embryos, and inflamed tissues: in situ analysis using a novel Il-33-LacZ gene trap reporter strain. J Immunol. 2012; 188(7):3488–95. [PubMed: 22371395]
14. Liew FY, Girard JP, Turnquist HR. Interleukin-33 in health and disease. Nature reviews Immunology. 2016; 16(11):676–89.
15. Cayrol C, Girard JP. IL-33: an alarmin cytokine with crucial roles in innate immunity, inflammation and allergy. Current opinion in immunology. 2014; 31:31–7. [PubMed: 25278425]
16. Drake LY, Kita H. IL-33: biological properties, functions, and roles in airway disease. Immunological reviews. 2017; 278(1):173–84. [PubMed: 28658560]
17. Shen JX, Liu J, Zhang GJ. Interleukin-33 in Malignancies: Friends or Foes? Frontiers in immunology. 2018; 9:3051. [PubMed: 30619376]
18. Liu L, Liu L, Yao HH, Zhu ZQ, Ning ZL, Huang Q. Stromal Myofibroblasts Are Associated with Poor Prognosis in Solid Cancers: A Meta-Analysis of Published Studies. PloS one. 2016; 11(7) e0159947 [PubMed: 27459365]
19. Cohen N, Shani O, Raz Y, Sharon Y, Hoffman D, Abramovitz L, et al. Fibroblasts drive an immunosuppressive and growth-promoting microenvironment in breast cancer via secretion of Chitinase 3-like 1. Oncogene. 2017; 36(31):4457–68. [PubMed: 28368410]
20. Erez N, Truitt M, Olson P, Arron ST, Hanahan D. Cancer-Associated Fibroblasts Are Activated in Incipient Neoplasia to Orchestrate Tumor-Promoting Inflammation in an NF-kappaB-Dependent Manner. Cancer cell. 2010; 17(2):135–47. [PubMed: 20138012]
21. Ershaid N, Sharon Y, Doron H, Raz Y, Shani O, Cohen N, et al. NLRP3 inflammasome in fibroblasts links tissue damage with inflammation in breast cancer progression and metastasis. Nat Commun. 2019; 10(1) 4375 [PubMed: 31558756]
22. Raz Y, Cohen N, Shani O, Bell RE, Novitskiy SV, Abramovitz L, et al. Bone marrow-derived fibroblasts are a functionally distinct stromal cell population in breast cancer. The Journal of experimental medicine. 2018; 215(12):3075–93. [PubMed: 30470719]
23. Shani O, Raz Y, Megides O, Shacham HNC, Silverbush D, et al. Evolution of metastases-associated fibroblasts in the lung microenvironment is driven by stage-specific transcriptional plasticity. bioRxiv. 2019 778936
24. Misharin AV, Morales-Nebreda L, Mutlu GM, Budinger GR, Perlman H. Flow cytometric analysis of macrophages and dendritic cell subsets in the mouse lung. American journal of respiratory cell and molecular biology. 2013; 49(4):503–10. [PubMed: 23672262]
25. Yu YR, O'Koren EG, Hotten DF, Kan MJ, Kopin D, Nelson ER, et al. A Protocol for the Comprehensive Flow Cytometric Analysis of Immune Cells in Normal and Inflamed Murine Non-Lymphoid Tissues. PloS one. 2016; 11(3) e0150606 [PubMed: 26938654]
26. Ma XJ, Dahiya S, Richardson E, Erlander M, Sgroi DC. Gene expression profiling of the tumor microenvironment during breast cancer progression. Breast cancer research : BCR. 2009; 11(1):R7. [PubMed: 19187537]
27. Finak G, Bertos N, Pepin F, Sadekova S, Souleimanova M, Zhao H, et al. Stromal gene expression predicts clinical outcome in breast cancer. Nature medicine. 2008; 14(5):518–27.
28. Gruosso T, Gigoux M, Manem VSK, Bertos N, Zuo D, Perlitch I, et al. Spatially distinct tumor immune microenvironments stratify triple-negative breast cancers. The Journal of clinical investigation. 2019; 129(4):1785–800. [PubMed: 30753167]
29. Xu J, Acharya S, Sahin O, Zhang Q, Saito Y, Yao J, et al. 14-3-3zeta turns TGF-beta's function from tumor suppressor to metastasis promoter in breast cancer by contextual changes of Smad partners from p53 to Gli2. Cancer cell. 2015; 27(2):177–92. [PubMed: 25670079]

30. Zhang XH, Wang Q, Gerald W, Hudis CA, Norton L, Smid M, et al. Latent bone metastasis in breast cancer tied to Src-dependent survival signals. Cancer cell. 2009; 16(1):67–78. [PubMed: 19573813]

31. Jovanovic IP, Pejnovic NN, Radosavljevic GD, Pantic JM, Milovanovic MZ, Arsenijevic NN, et al. Interleukin-33/ST2 axis promotes breast cancer growth and metastases by facilitating intratumoral accumulation of immunosuppressive and innate lymphoid cells. International journal of cancer Journal international du cancer. 2014; 134(7):1669–82. [PubMed: 24105680]

32. Li J, Liu C, Chen Y, Gao C, Wang M, Ma X, et al. Tumor Characterization in Breast Cancer Identifies Immune-Relevant Gene Signatures Associated With Prognosis. Front Genet. 2019; 10:1119. [PubMed: 31781173]

33. Martin NT, Martin MU. Interleukin 33 is a guardian of barriers and a local alarmin. Nature immunology. 2016; 17(2):122–31. [PubMed: 26784265]

34. Pinto SM, Subbannayya Y, Rex DAB, Raju R, Chatterjee O, Advani J, et al. A network map of IL-33 signaling pathway. J Cell Commun Signal. 2018; 12(3):615–24. [PubMed: 29705949]

35. De la Fuente M, MacDonald TT, Hermoso MA. The IL-33/ST2 axis: Role in health and disease. Cytokine & growth factor reviews. 2015; 26(6):615–23. [PubMed: 26271893]

36. Dahlgren MW, Jones SW, Cautivo KM, Dubinin A, Ortiz-Carpena JF, Farhat S, et al. Adventitial Stromal Cells Define Group 2 Innate Lymphoid Cell Tissue Niches. Immunity. 2019; 50(3):707–22. e6 [PubMed: 30824323]

37. Mahlakoiv T, Flamar AL, Johnston LK, Moriyama S, Putzel GG, Bryce PJ, et al. Stromal cells maintain immune cell homeostasis in adipose tissue via production of interleukin-33. Sci Immunol. 2019; 4(35)

38. Chen SF, Nieh S, Jao SW, Wu MZ, Liu CL, Chang YC, et al. The paracrine effect of cancer-associated fibroblast-induced interleukin-33 regulates the invasiveness of head and neck squamous cell carcinoma. The Journal of pathology. 2013; 231(2):180–9. [PubMed: 23775566]

39. Zhou Q, Wu X, Wang X, Yu Z, Pan T, Li Z, et al. The reciprocal interaction between tumor cells and activated fibroblasts mediated by TNF-alpha/IL-33/ST2L signaling promotes gastric cancer metastasis. Oncogene. 2019

40. Andersson P, Yang Y, Hosaka K, Zhang Y, Fischer C, Braun H, et al. Molecular mechanisms of IL-33-mediated stromal interactions in cancer metastasis. JCI Insight. 2018; 3(20)

41. Yang Y, Andersson P, Hosaka K, Zhang Y, Cao R, Iwamoto H, et al. The PDGF-BB-SOX7 axis-modulated IL-33 in pericytes and stromal cells promotes metastasis through tumour-associated macrophages. Nat Commun. 2016; 7 11385 [PubMed: 27150562]

42. Johnston LK, Hsu CL, Krier-Burris RA, Chhiba KD, Chien KB, McKenzie A, et al. IL-33 Precedes IL-5 in Regulating Eosinophil Commitment and Is Required for Eosinophil Homeostasis. Journal of Immunology. 2016; 197(9):3445–53.

43. Afferni C, Buccione C, Andreone S, Galdiero MR, Varricchi G, Marone G, et al. The Pleiotropic Immunomodulatory Functions of IL-33 and Its Implications in Tumor Immunity. Frontiers in immunology. 2018; 9:2601. [PubMed: 30483263]

44. Baker KJ, Houston A, Brint E. IL-1 Family Members in Cancer; Two Sides to Every Story. Frontiers in immunology. 2019; 10:1197. [PubMed: 31231372]

45. Fournie JJ, Poupot M. The Pro-tumorigenic IL-33 Involved in Antitumor Immunity: A Yin and Yang Cytokine. Frontiers in immunology. 2018; 9:2506. [PubMed: 30416507]

46. Jin Z, Lei L, Lin D, Liu Y, Song Y, Gong H, et al. IL-33 Released in the Liver Inhibits Tumor Growth via Promotion of CD4(+) and CD8(+) T Cell Responses in Hepatocellular Carcinoma. J Immunol. 2018; 201(12):3770–79. [PubMed: 30446569]

47. Dominguez D, Ye C, Geng Z, Chen S, Fan J, Qin L, et al. Exogenous IL-33 Restores Dendritic Cell Activation and Maturation in Established Cancer. J Immunol. 2017; 198(3):1365–75. [PubMed: 28011934]

48. Qi L, Zhang Q, Miao Y, Kang W, Tian Z, Xu D, et al. Interleukin-33 activates and recruits natural killer cells to inhibit pulmonary metastatic cancer development. International journal of cancer Journal international du cancer. 2020; 146(5):1421–34. [PubMed: 31709531]

49. Lawrence MG, Steinke JW, Borish L. Cytokine-targeting biologics for allergic diseases. Annals of allergy, asthma & immunology : official publication of the American College of Allergy, Asthma, & Immunology. 2018; 120(4):376–81.

50. Taranova AG, Maldonado D 3rd, Vachon CM, Jacobsen EA, Abdala-Valencia H, McGarry MP, et al. Allergic pulmonary inflammation promotes the recruitment of circulating tumor cells to the lung. Cancer research. 2008; 68(20):8582–9. [PubMed: 18922934]

Europe PMC Funders Author Manuscripts

Europe PMC Funders Author Manuscripts

Significance

This study elucidates a novel role for fibroblast-derived IL-33 in facilitating breast cancer lung metastasis by modifying the immune microenvironment at the metastatic niche towards type-2 inflammation.

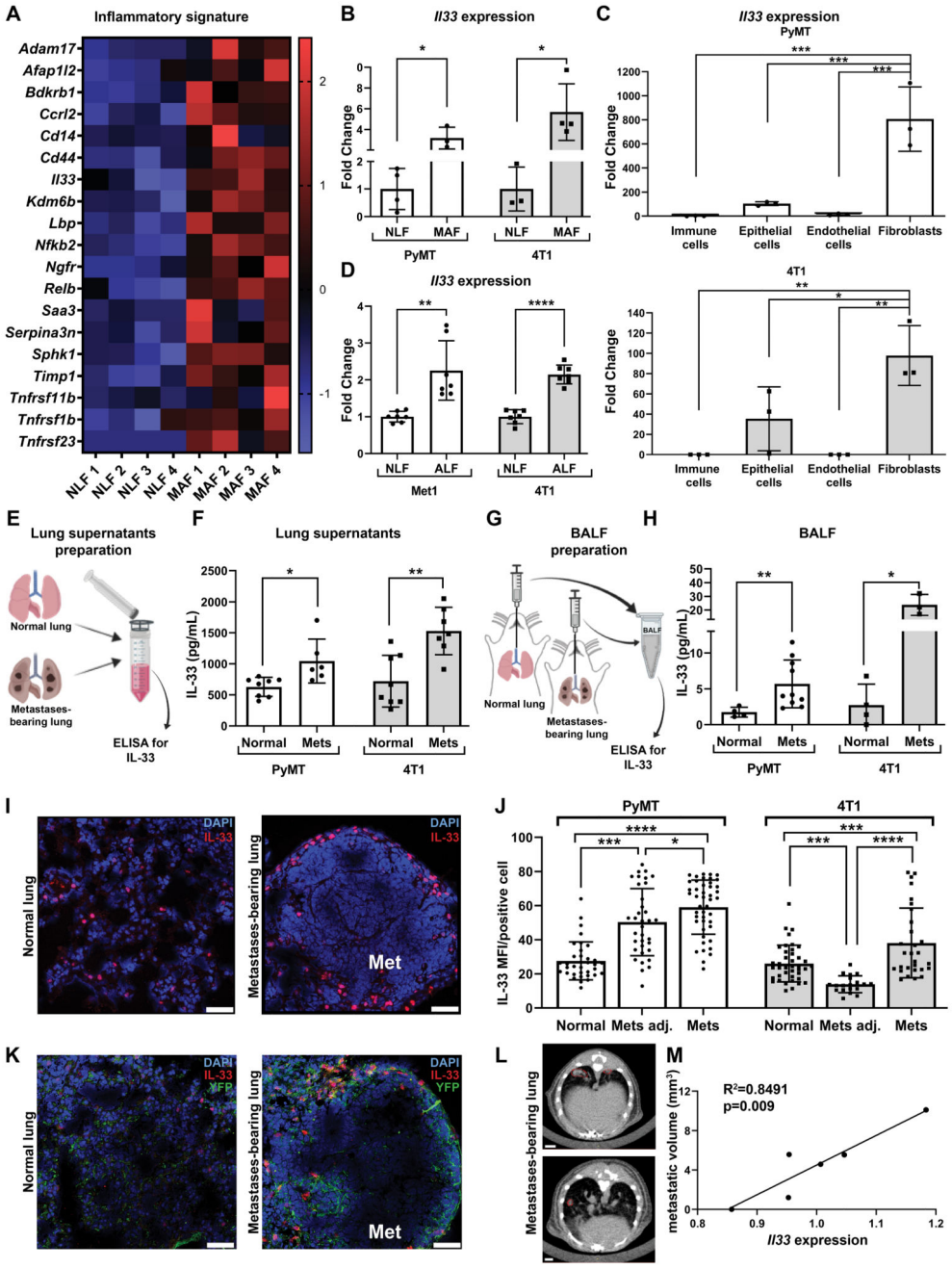

Figure 1. IL-33 is upregulated in metastases-associated fibroblasts at the lung metastatic microenvironment.

(A) Heatmap of inflammatory genes that were enriched in an unbiased GO analysis (GO:0006954, FDR=0.00045). Analysis was performed on genes significantly upregulated in MAF vs. NLF (FC>1.5, adjusted *P*<0.05). **(B)** Expression of *Il33* in NLF and MAF sorted from MMTV-PyMT;*Col1a1-YFP* transgenic mice (n=3) vs. normal FVB/n;Col1a1-YFP controls (n=4) and BALB/c;Col1a1-YFP mice bearing 4T1 metastases (n=4) vs. BALB/c;Col1a1-YFP controls (n=3). Data are presented as fold change ± SD. Welch's t-test,

*p<0.05. **(C)** qRT-PCR analysis of *Il33* expression in FACS sorted lung cell populations. Cells were isolated from MMTV-PyMT;Col1a1-YFP mice (n=3) or BALB/c;Col1a1-YFP mice bearing 4T1 tumor cell metastases (n=3). Data presented as mean ± SD, normalized to control immune cells; one-way ANOVA followed by Tukey's multiple comparisons test. *p<0.05, **p<0.01, ***p<0.001. **(D)** qRT-PCR analysis of *Il33* expression. White bars: FVB/n lung fibroblasts incubated with SFM (NLF, n=7) or with Met1 tumor cells CM (ALF- activated lung fibroblasts, n=6). Gray bars: BALB/c NLF incubated with SFM (n=7) or ALF (n=7) incubated with 4T1 tumor cells CM. Data presented as mean ± SD; Welch's t-test. **P<0.01, ****p<0.0001. **(E)** Scheme of IL-33 ELISA in lung homogenate supernatants. **(F)** Quantification of IL-33 ELISA presented in E: FVB/n normal lungs (n=7) vs. MMTV-PyMT metastases-bearing lungs (Mets, n=6) and BALB/c normal lungs (n=8) vs. BALB/c mice bearing 4T1 metastases (n=7). Data presented as mean ±SD; Welch's t-test. *P<0.05. **P<0.01. **(G)** Scheme of IL-33 ELISA in BALF. **(H)** Quantification of IL-33 ELISA presented in G: FVB/n normal lungs (n=4) vs. MMTV-PyMT metastases-bearing lungs (n=10) and BALB/c normal lungs (n=4) vs. BALB/c mice bearing 4T1 metastases (n=3). Data presented as mean ± SD; Welch's *t*-test. *P<0.05, **P<0.01. **(I)** Representative images of IL-33 immunofluorescence staining in lungs. n=3 mice per group; Scale bars, 50μm. Cell nuclei, DAPI; IL-33, Rhodamine Red. **(J)** Quantification of mean fluorescent intensity (MFI) per IL33+ positive cell in staining performed in (I). FVB/n normal lungs vs. PyMT metastases-bearing lungs, and BALB/c normal lungs vs. mice bearing 4T1 lung metastases. 6-8 fields of view - FOV/lung were analyzed. Mets adj: lung areas without metastases, Mets: metastases. One-way ANOVA with Tukey's correction for multiple comparisons. *P<0.05, **P<0.01, ***P<0.001, ****P<0.0001. **(K)** Representative images of IL-33 and YFP immunofluorescence staining in lungs. n=3 mice per group; Scale bars, 50μm. Cell nuclei, DAPI; IL-33, Rhodamine Red; YFP, Alexa Fluor-488 **(L)** Representative CT imaging of 4T1 lung metastasis. Metastases are marked in red. n=4. **(M)** Pearson correlation analysis between metastatic volume (mm^3) measured by CT imaging presented in (L) and *Il33* expression analyzed by qRT-PCR in total lungs.

Europe PMC Funders Author Manuscripts

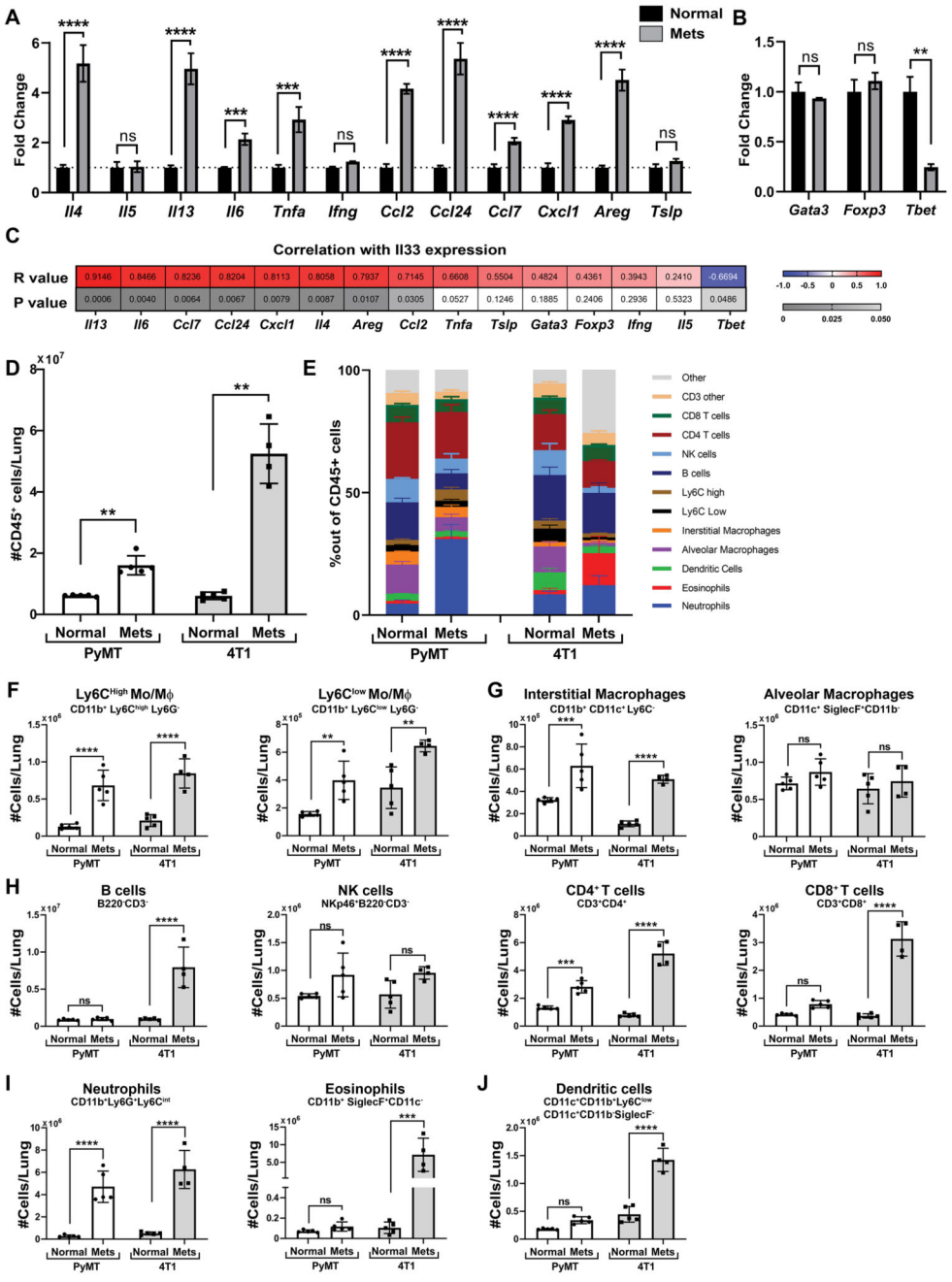

Figure 2. Lung metastases formation is characterized by extensive modifications in the immune milieu.

(A,B) qRT-PCR analysis of *Il33* downstream genes (A) and immune related TFs (B) in total lungs derived from BALB/c mice bearing 4T1 tumor cell metastases (n=4) and in normal controls (n=5). Data are presented as mean ± SD of technical repeats; Multiple t-tests with Welch's correction, FDR(Q)=5% and Fold Change>1.5. ***q*<0.01, ****q*<0.001, *****q*<0.0001. ns-not significant. **(C)** Heat map presenting Pearson correlation analysis between *Il33* expression and the expression of the genes presented in (A,B). Results are

presented as Pearson R values and P values per gene. Significant results were considered as $P<0.05$ and $R>$I0.651 **(D)** Flow cytometry analysis of the number of immune cells in normal lungs and metastases bearing lungs derived from FVB/n normal lungs (Normal, n=5) vs. MMTV-PyMT metastases-bearing lungs (Mets, n=5) and BALB/c normal lungs (n=5) vs. BALB/c mice bearing 4T1 tumor cell metastases following orthotopic injection (n=4). Data presented as mean ± SD. Welch's *t*-test, $^{**}P<0.01$. **(E)** Quantification of flow cytometry analysis of immune cell populations in the lung derived from FVB/n normal lungs (Normal, n=5) vs. MMTV-PyMT metastases-bearing lungs (Mets, n=5) and BALB/c normal lungs (n=5) vs. BALB/c mice bearing 4T1 tumor cell metastases following orthotopic injection (n=4). Data presented as mean ± SD of percent out of $CD45^+$ cells. Gating strategy presented in Supplementary Fig. S2C,D. **(F-J)** Cell numbers of different populations based on quantification performed in (E), Monocytes presented in (F), Macrophages presented in (G), Lymphoid cells presented in (H), granulocytes presented in (I), Dendritic cells in (J), Two-way ANOVA with Sidak's correction for multiple comparisons. $^{**}P<0.01$, $^{***}P<0.001$ $^{****}P<0.0001$.

Europe PMC Funders Author Manuscripts

Europe PMC Funders Author Manuscripts

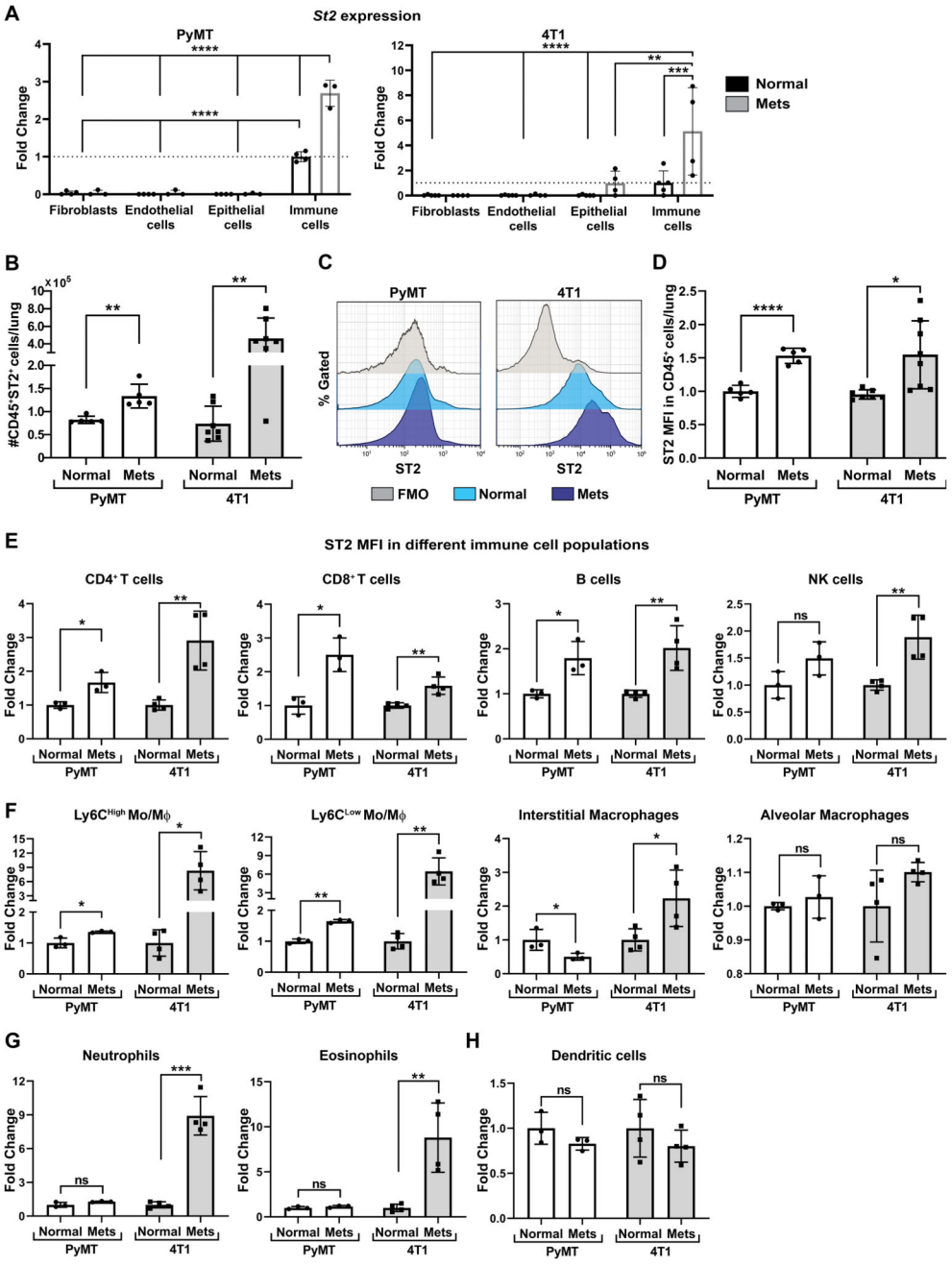

Figure 3. ST2, the IL-33 receptor is highly upregulated in immune cells at the metastatic microenvironment

(A) qRT-PCR analysis of *St2* expression in FACS sorted lung cell populations: immune cells ($CD45^+CD31^-$), endothelial cells ($CD31^+CD45^-$), epithelial/tumor cells ($EpCAM^+CD45^-CD31^-$) or fibroblasts ($YFP^+CD45^-CD31^-EpCAM^-$). Cells were sorted by flow cytometry from MMTV-PyMT;*Col1a1*-YFP mice (n=3), FVB/n;*Col1a1*-YFP (n=4) or BALB/c;Col1a1-YFP mice bearing 4T1 tumor cell metastases (n=4) or normal BALB/c;*Col1a1*-YFP control (n=5). Data presented as mean ±SD normalized to control immune cells; one-way analysis of variance followed by Tukey's multiple comparisons test. $^{**}p<0.01$, $^{***}p<$

Europe PMC Funders Author Manuscripts

0.001, **** p <0.0001. **(B)** Flow cytometric analysis of the number of $ST2^{+}CD45^{+}$ immune cells in FVB/n normal lungs (n=5) vs. MMTV-PyMT metastases-bearing lungs (n=5) and BALB/c normal lungs (n=7) vs. BALB/c mice bearing 4T1 tumor cell metastases following orthotopic injection (n=7). Data presented as mean ±SD; Welch's t-test **P<0.01. **(C)** Flow cytometry representative histogram of ST2 fluorescent intensity (MFI) out of total $CD45^{+}$ immune cells in normal lungs and metastases-bearing lungs (Mets). Histograms of Normal and Mets represent individual mice. FMO-fluorescent minus one. **(D)** Quantification of flow cytometric analysis presented in (C). Each sample was normalized to FMO control and to normal control. Welch's t-test, *P<0.05, ****p<0.0001. **(E-H)** Flow cytometric analysis of ST2 fluorescence intensity in immune cell populations in normal lungs and metastases-bearing lungs derived from FVB/n normal lungs (n=3) vs. MMTV-PyMT metastases-bearing lungs (n=3) and from BALB/c mice injected with 4T1 tumor cells (n=4) or control BALB/c mice (n=4). Lymphoid cells (E), Monocytes or Macrophages (F), Granulocytes (G), Dendritic cells (H). Gating strategy presented in Supplementary Fig. S2C,D. Each cell population was normalized to FMO control and to normal control. Multiple t-tests with Welch's correction, FDR(Q)=5%. *q<0.05, **q<0.01, ***q<0.001, ns-not significant.

Europe PMC Funders Author Manuscripts

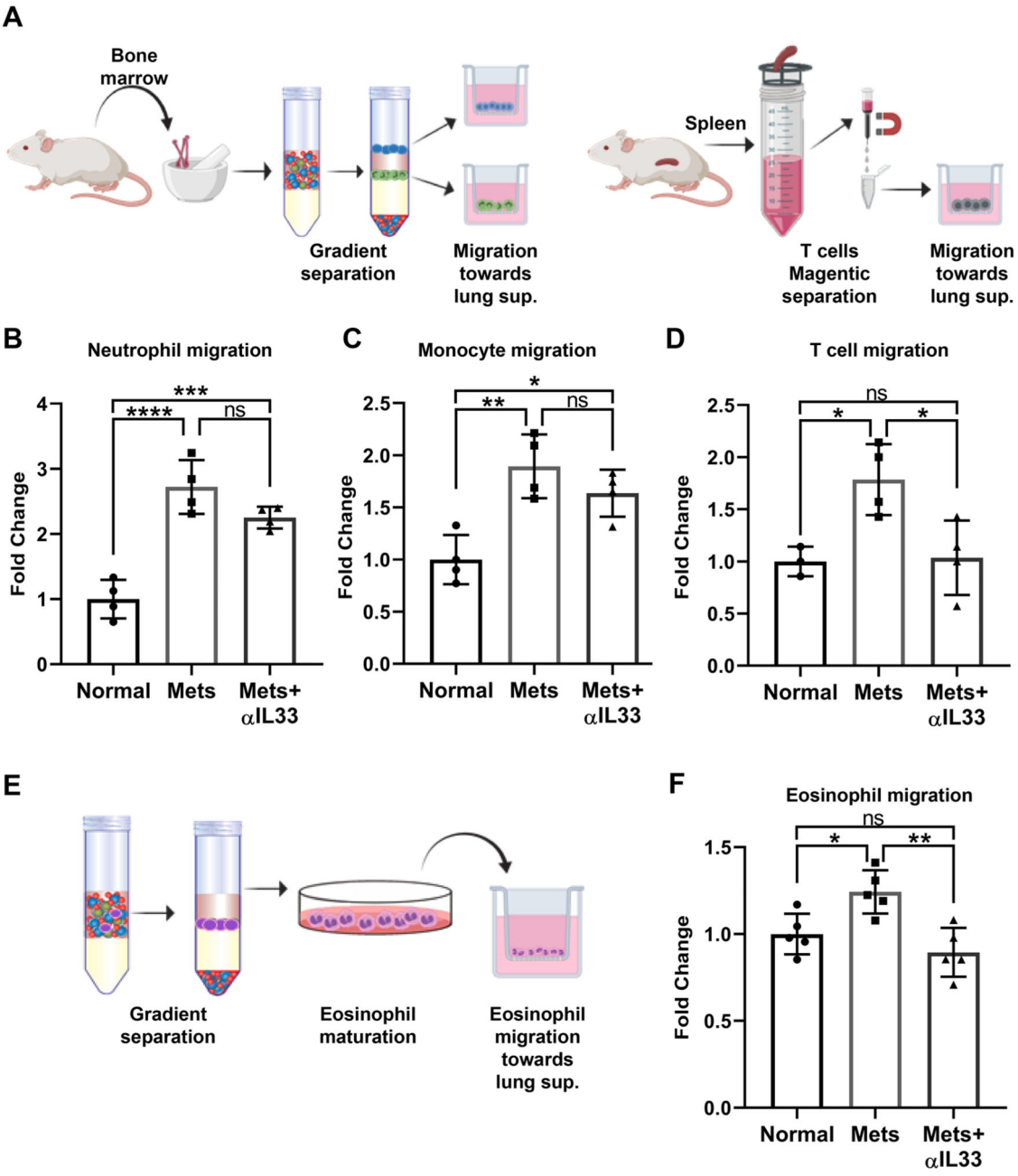

Figure 4. IL-33 is functionally important for direct recruitment of T cells and eosinophils.

(A) Scheme for *in vitro* migration assays of neutrophil, monocyte and T cells. Bone marrow-derived neutrophils and monocytes were isolated by gradient separation. $CD3^+$ T cells were purified from spleen. **(B-D)** Quantification of neutrophil (B) monocytes (C) and T cells (D) migration based on experimental design described in (a). One-way ANOVA with Tukey's correction for multiple comparisons tests. **P*<0.05, ***P* <0.01, ****P*<0.001, *****P*<0.0001. **(E)** Scheme for eosinophil isolation and *in vitro* maturation, followed by migration assay. Eosinophil purity analysis is presented in Supplementary Fig. S3. **(F)** Quantification of

eosinophils migration. One-way ANOVA with Tukey's correction for multiple comparisons tests. *P<0.05, **P <0.01.

Europe PMC Funders Author Manuscripts

Europe PMC Funders Author Manuscripts

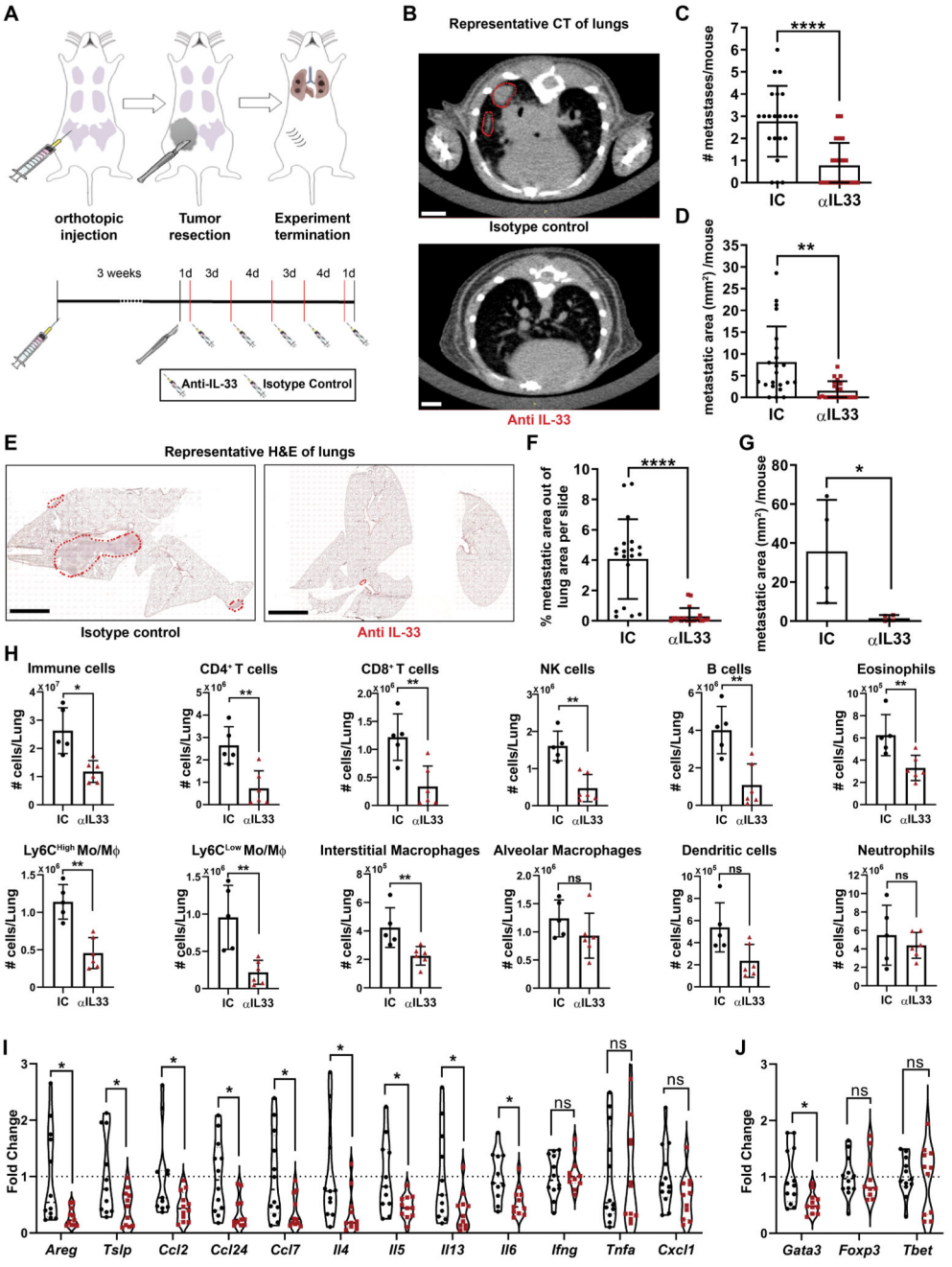

Figure 5. Inhibition of IL-33 attenuates lung metastases, and tempers type-2 immunity in the metastatic lung.

(A) Experimental design of IL-33 inhibition *in vivo.* Experiments were performed 5 separate times with at least n=5 mice per group. **(B)** Representative CT scans of mice injected as described in (A). Metastases are circled in red. Scale bars: 3mm. (IC: isotype control, αIL33: Anti-IL33 Antibody). **(C)** Number of metastatic foci as identified by CT scans. Welch's *t*-test, ****$P<0.0001$. **(D)** Area of metastases per mouse as measured by CT scans. Welch's *t*-test, **$P<0.01$. **(E)** Representative H&E staining of lungs injected as described in

(A), metastases are circled in red. Scale bars: 3mm **(F)** Quantification of H&E staining for the metastatic area out of total lung area (metastatic burden). n=19 lung tissue sections of 4 mice. Welch's t-test, ****P<0.0001. **(G)** Quantification of H&E staining metastatic area per mouse. n=4 mice. Welch's one-tailed t-test, *P<0.05. **(H)** Flow cytometry Immune cell populations analysis in mice injected as described in (A). Multiple t-tests with Welch's correction, FDR(Q)= 1%. *q<0.05, **q<0.01, ****q<0.0001. **(I,J)** Expression analysis by qRT-PCR of selected genes in lungs derived from mice injected with α-IL-33 or with IC, as described in (a). n≥11 mice per group. Multiple t-tests with Welch's correction, FDR(Q)=5%. *q<0.05, **q<0.01, ns-not significant.

Europe PMC Funders Author Manuscripts

Europe PMC Funders Author Manuscripts

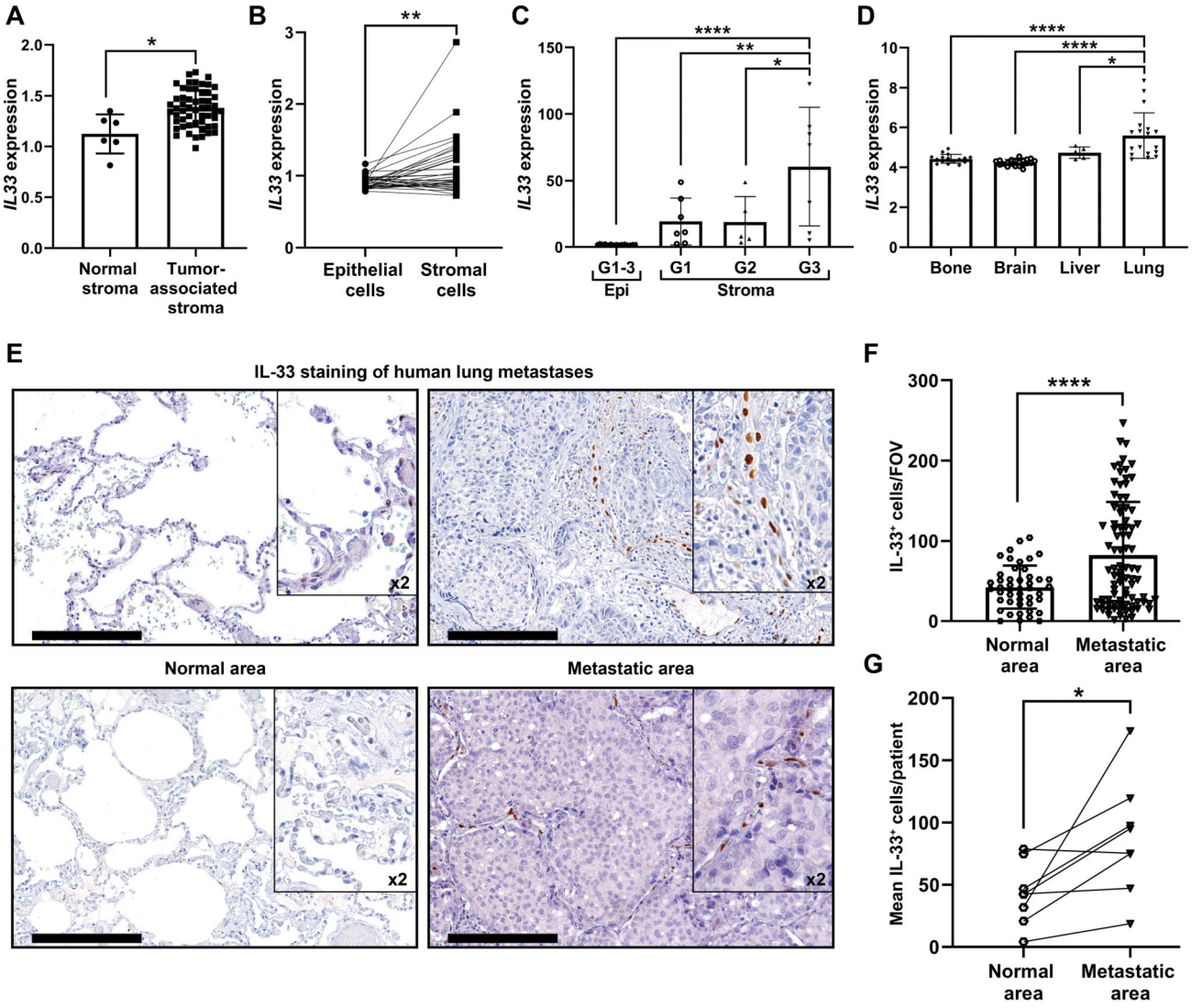

Figure 6. IL-33 is upregulated in the stroma of breast cancer primary tumors and lung metastases in human patients.

(A) *IL33* expression in tumor-associated stroma as compared with normal stroma from GSE9014. Welch's *t*-test, **P*<0.05. **(B)** *IL33* expression in paired patient samples of epithelial cells and tumor-associated stroma in primary breast tumors from GSE88715. Paired t-test. ***P*<0.01. **(C)** *IL33* expression in primary breast-tumor tissue (Epi) and tumor associated-stroma (Stroma) from GSE14548. Stromal expression is divided into tumor grade (Stroma-grade 1: G1; Stroma-grade 2: G2; Stroma-grade 3: G3). For the epithelial expression of *IL33* all grades were combined (G1-3). One-way ANOVA with Tukey's correction for multiple comparisons, **P*<0.05, ***P*<0.01, *****P*<0.0001. **(D)** *IL33* mRNA expression in human breast cancer metastasis from different metastatic sites. Data was derived from GSE14020. One-way ANOVA with Tukey's correction for multiple comparisons tests. **P*<0.05, **** *P*< 0.0001. **(E)** Representative IHC staining of IL-33 in lung metastases of breast cancer patients (n=8). Normal areas (remote from metastatic foci)

were quantified as controls. Scale bars: 200μm. **(F)** Quantification of the number of IL-33+ cells per FOV in IHC performed in (c). 10-15 FOV/section. Data presented as mean ±SD; Welch's *t*-test. ****$P<0.0001$. **(G)** Analysis of the mean IL-33+ cells/patient, compared with paired adjacent normal lung tissue. n=8; Paired *t*-test. *$P<0.05$.

Europe PMC Funders Author Manuscripts